Quantitative Analysis of Collagen Lamellae in the Normal and Keratoconic Human Cornea by Second Harmonic Generation Imaging Microscopy

Naoyuki Morishige,[1] Ryutaro Shin-gyou-uchi,[1] Haruya Azumi,[1] Hiroaki Ohta,[1] Yukiko Morita,[1] Naoyuki Yamada,[1] Kazuhiro Kimura,[1] Atsushi Takahara,[2] and Koh-Hei Sonoda[1]

[1]Department of Ophthalmology, Yamaguchi University Graduate School of Medicine, Ube, Yamaguchi, Japan
[2]Institute for Materials Chemistry and Engineering, Kyushu University, Fukuoka, Fukuoka, Japan

Correspondence: Naoyuki Morishige, Department of Ophthalmology, Yamaguchi University Graduate School of Medicine, 1-1-1 Minami Kogushi, Ube, Yamaguchi 755-8505, Japan;
morishig@yamaguchi-u.ac.jp.

Submitted: July 29, 2014
Accepted: November 4, 2014

Citation: Morishige N, Shin-gyou-uchi R, Azumi H, et al. Quantitative analysis of collagen lamellae in the normal and keratoconic human cornea by second harmonic generation imaging microscopy. *Invest Ophthalmol Vis Sci*. 2014;55:8377–8385. DOI:10.1167/iovs.14-15348

Purpose. To characterize the structural properties of collagen lamellae in the normal and keratoconic human corneal stroma, we measured their width and angle relative to Bowman's layer (BL).

Methods. Thirteen normal and four keratoconic corneas were examined. Collagen lamellae in tissue blocks from the central cornea were visualized by second harmonic generation imaging microscopy. Images obtained in 1-μm steps from BL to Descemet's membrane (DM) were subjected to three-dimensional reconstruction. The reconstructed data sets were divided into 10 layers of equal depth (L1–L10) for analysis. The width of lamellae adherent to BL (L0) was also determined.

Results. For the normal cornea, the width (mean ± SD) of collagen lamellae was 6.5 ± 1.7 μm at L0, decreased to 4.3 ± 1.3 μm at L1, and then increased gradually with progression toward DM to 122.2 ± 34.5 μm at L10, whereas the angle of lamellae was 20.9° ± 5.4° at L1 and decreased initially to 10.6° ± 3.2° at L2 before declining gradually to 2.7° ± 2.2° at L10. The width and angle of collagen lamellae in the keratoconic cornea were significantly larger and smaller, respectively, relative to those in the normal cornea.

Conclusions. In the normal human cornea, collagen lamellae adjacent to BL are narrow and form a steep angle with BL, whereas they increase in width and their angle relative to BL flattens with progression toward DM. These properties of collagen lamellae are altered in keratoconus and are likely related to abnormalities of corneal shape.

Keywords: corneal stroma, collagen, normal cornea, second harmonic generation, keratoconus

The transparency of the corneal stroma is essential for vision and is dependent on the well-organized structure of collagen within this tissue. Disruption of this structure of stromal collagen associated with various corneal diseases thus results in corneal opacity and a consequent loss of visual acuity. In addition to the importance of its transparency, the corneal stroma must be sufficiently rigid to maintain corneal shape, another key determinant of visual acuity that is dependent on stromal collagen structure. The corneal stroma contains collagen of types I, V, VI, XII, and XIV,[1] and the collagen fibrils align with the same orientation to form lamellae. Electron microscopy has revealed that these collagen lamellae in the human corneal stroma vary in width from 0.5 to 250 μm and in thickness from 0.2 to 2.5 μm,[2] and that they are interwoven with each other at various angles.[3] The lamellae extend from limbus to limbus,[4] and x-ray scattering analysis has shown that they change direction as they course from the center to the outer zone of the cornea.[5] We have previously described the three-dimensional (3D) interwoven structure of collagen lamellae at the anterior stroma of the normal human cornea as revealed by second harmonic generation (SHG) imaging microscopy.[6,7] A key advantage of this approach is that it allows evaluation of the structural characteristics of collagen lamellae in 3D data sets. For example, the angle of collagen lamellae relative to Bowman's layer is not evaluable by analysis of sectioned specimens because the lamellae course in various directions.[6,7] Second harmonic generation imaging microscopy allows quantitative analysis of the angle of collagen lamellae.[7]

Keratoconus is a relatively common condition characterized by progressive corneal protrusion and thinning that result in reduced visual acuity as well as in difficulty in the wearing of contact lenses. Although various cytokines,[8,9] matrix metalloproteinases,[10–12] and oxidative stress[13–15] have been implicated in its pathogenesis, the mechanisms responsible for the development of keratoconus have remained unclear. The anatomy of the keratoconic cornea has been investigated by electron microscopy,[16–18] and x-ray scattering analysis has implicated slippage of collagen lamellae in the etiology of keratoconus.[19,20] Second harmonic generation analysis of the keratoconic cornea has revealed altered collagen lamellae and fibrils[21,22] as well as a loss of the normal interwoven structure of the lamellae.[23]

Given that the 3D structure of collagen lamellae throughout the entire thickness of the corneal stroma has not previously been determined in detail, we have evaluated the 3D characteristics of collagen lamellae from the anterior to the

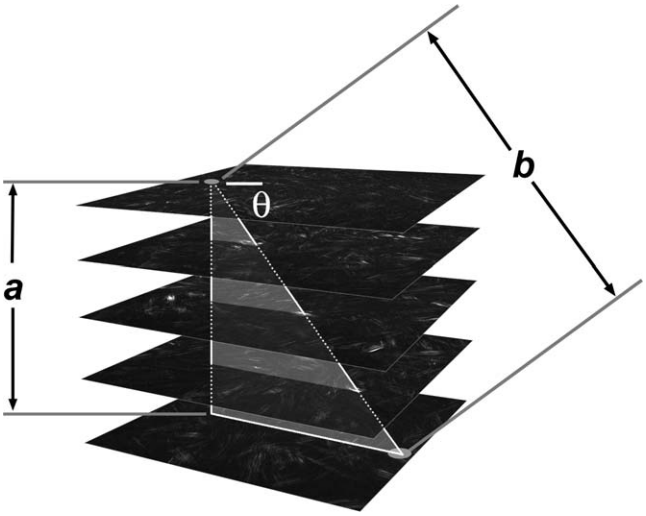

FIGURE 1. Measurement of the angle of collagen lamellae. The angle (θ) is provided by $\sin^{-1}(a/b)$, where height a is given by the number of planes in the continuously scanned SHG images and length b is measured with the use of ZEN software.

posterior region of the normal and keratoconic human corneal stroma.

METHODS

Specimens

The study was approved by the Institutional Review Board of Yamaguchi University Hospital and adhered to the tenets of the Declaration of Helsinki. We obtained 11 human sclerocorneal specimens directly from Sight Life Eye Bank (Seattle, WA, USA), and two such specimens originally obtained from the eye bank were kindly provided by A. Kobayashi (Kanazawa University, Japan). The 13 specimens were derived from six men and seven women ranging in age from 43 to 75 years (mean ± SD, 60.2 ± 10.2). Four keratoconic corneas (from two men and two women with a mean ± SD age of 51.5 ± 13.9 years and age range of 38–64 years) were obtained at the time of penetrating keratoplasty performed at Yamaguchi University Hospital. The tissue was immediately fixed overnight at 4°C in 4% paraformaldehyde, after which blocks of ~2 mm^2 were dissected from the central region, washed with phosphate-buffered saline, mounted on glass coverslips with 50% glycerol in phosphate-buffered saline, and imaged. Tissue blocks from the midperipheral region of the cornea were also examined in the case of the keratoconic specimens.

SHG Imaging Microscopy

Second harmonic generation imaging microscopy was performed as described previously.[6] Samples were initially observed with an Axiovert 200 microscope (Zeiss, Jena, Germany) equipped with a ×40 (numerical aperture = 1.2) water-immersion objective lens (Zeiss). Two-photon second harmonic signals from collagen were generated with a mode-locked titanium:sapphire laser (Chameleon; Coherent, Santa Clara, CA, USA). The optimal wavelength for the generation of second harmonic signals from human corneal collagen was previously found to be 800 nm.[6] Forward scatter–transmitted signals as SHG forward signal that passed through the tissue were collected with the use of a condenser lens (numerical aperture = 0.55) and a narrow bandpass filter (400/50) positioned in front of the transmission light detector of a laser confocal microscope (LSM 710NLO2; Zeiss). The samples were mounted with the corneal surface parallel to the scanning plane and were scanned with a step size of 1 μm in the z-axis, extending from the surface of Descemet's membrane to that of Bowman's layer. Twelve-bit, 512 by 512 images were recorded. The 3D data sets were analyzed with the use of ZEN 2011

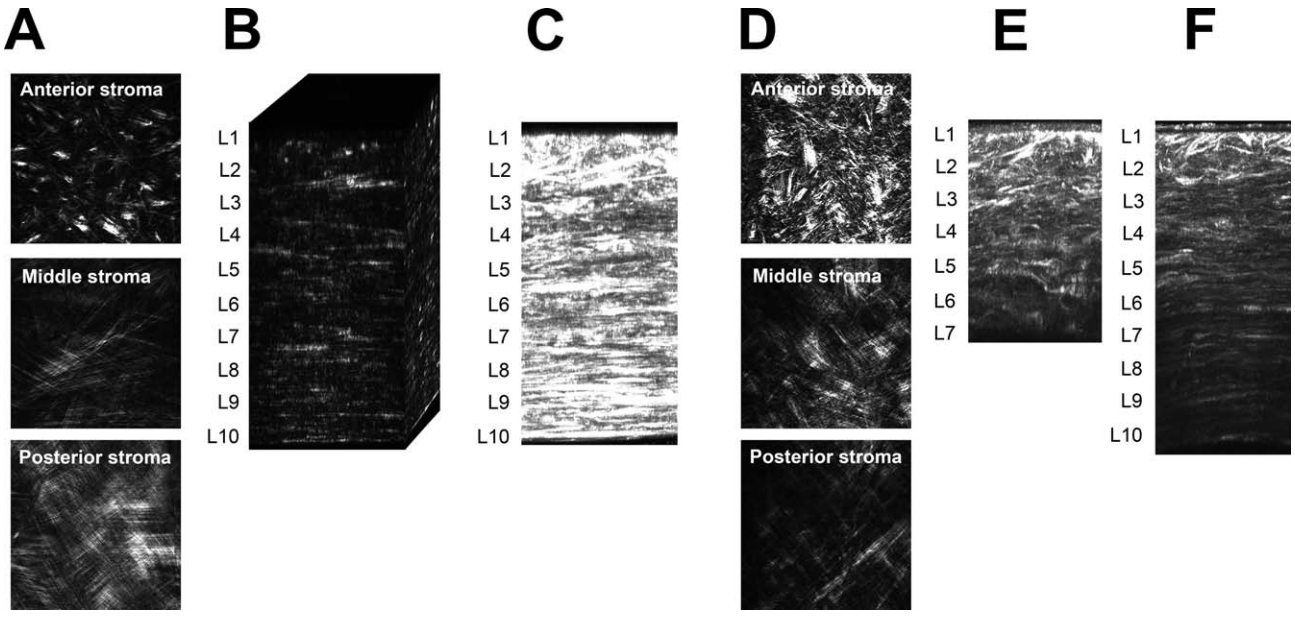

FIGURE 2. Obtained SHG images and reconstructed images of collagen lamellae in the normal and keratoconic corneal stroma. (**A**) SHG images of a single plane obtained from anterior, middle, or posterior regions of the normal stroma. The images are equivalent to frontal sections of the corneal stroma. (**B**) Side view of stacked SHG images of the normal stroma. Assigned layers L1 to L10 are indicated. (**C**) Projection of stacked SHG images of the normal stroma. Note that collagen lamellae at the anterior stroma (L1–L3) are dense and interwoven. (**D**) SHG images of a single plane obtained from anterior, middle, or posterior regions of the keratoconic stroma. (**E**, **F**) Projection of stacked SHG images from the central (**E**) and midperipheral (**F**) regions of the keratoconic cornea.

Investigative Ophthalmology & Visual Science

TABLE 1. Width of Collagen Lamellae (μm) in Normal Subjects

Age/Sex	L0	L1	L2	L3	L4	L5	L6	L7	L8	L9	L10
48/F	7.2 ± 1.4	4.2 ± 0.6	12.5 ± 4.7	23.8 ± 3.4	29.6 ± 3.8	47.4 ± 6.2	67.7 ± 21.9	75.2 ± 19.6	84.0 ± 18.9	103.4 ± 34.0	123.7 ± 33.1
57/M	6.5 ± 1.5	4.5 ± 0.7	9.3 ± 2.3	21.6 ± 10.0	27.7 ± 11.5	38.8 ± 10.1	53.4 ± 19.2	72.4 ± 14.0	100.3 ± 57.5	128.8 ± 52.0	165.5 ± 60.7
57/M	6.9 ± 1.6	4.4 ± 0.7	6.7 ± 2.6	8.8 ± 3.5	27.8 ± 5.9	40.6 ± 14.1	63.7 ± 12.7	70.6 ± 13.5	98.0 ± 9.5	109.1 ± 12.8	116.4 ± 18.9
65/M	7.2 ± 2.5	2.6 ± 0.3	7.0 ± 0.3	13.6 ± 13.2	22.8 ± 10.6	45.8 ± 14.8	56.9 ± 6.4	64.0 ± 12.2	76.7 ± 25.9	106.8 ± 38.7	120.8 ± 39.3
68/M	7.0 ± 1.6	4.1 ± 0.4	17.8 ± 7.3	25.7 ± 12.9	41.9 ± 17.6	63.9 ± 24.7	67.0 ± 25.7	75.3 ± 13.8	81.7 ± 14.3	98.0 ± 26.3	107.2 ± 13.9
69/F	4.2 ± 1.6	3.7 ± 0.5	5.6 ± 1.4	15.5 ± 1.2	32.3 ± 4.7	55.7 ± 6.1	70.6 ± 8.6	88.8 ± 6.8	126.6 ± 7.2	166.8 ± 5.5	190.6 ± 7.7
69/M	7.1 ± 1.4	3.4 ± 1.7	7.3 ± 2.8	10.4 ± 3.8	21.3 ± 6.4	32.1 ± 8.8	47.0 ± 4.7	66.2 ± 10.6	62.1 ± 15.9	70.3 ± 9.5	87.4 ± 5.9
43/F	6.3 ± 1.2	4.0 ± 0.4	21.3 ± 2.7	31.7 ± 5.6	50.3 ± 6.6	75.7 ± 8.2	76.1 ± 22.3	81.8 ± 5.6	88.8 ± 2.4	104.3 ± 28.2	105.2 ± 16.4
69/M	5.9 ± 1.5	4.3 ± 1.3	13.5 ± 2.4	22.4 ± 3.7	28.5 ± 11.1	40.5 ± 10.4	54.4 ± 15.1	68.3 ± 10.7	86.8 ± 9.2	111.8 ± 12.7	133.5 ± 6.3
63/F	6.2 ± 0.7	2.7 ± 0.3	9.4 ± 2.3	18.4 ± 2.1	33.1 ± 4.2	35.3 ± 4.0	43.7 ± 9.1	52.0 ± 8.4	60.0 ± 13.2	82.5 ± 9.1	98.9 ± 3.8
48/F	6.7 ± 1.9	6.2 ± 1.2	12.2 ± 1.9	38.3 ± 17.3	44.6 ± 10.3	60.1 ± 21.8	66.1 ± 5.4	79.5 ± 7.7	88.1 ± 8.1	91.5 ± 15.0	114.9 ± 28.2
75/F	6.2 ± 1.8	6.7 ± 1.6	8.4 ± 2.5	26.8 ± 5.3	39.7 ± 9.7	51.2 ± 7.7	67.2 ± 5.0	71.7 ± 12.8	84.6 ± 11.6	86.8 ± 13.2	113.7 ± 25.9
69/F	7.2 ± 1.6	4.8 ± 1.1	14.8 ± 5.9	19.6 ± 4.0	23.6 ± 3.6	37.3 ± 9.8	53.6 ± 11.6	57.4 ± 14.7	60.1 ± 20.8	86.1 ± 9.9	111.1 ± 14.9
Overall mean ± SD	6.5 ± 1.7	4.3 ± 1.3	11.2 ± 5.3	21.3 ± 10.3	32.6 ± 12.4	48.0 ± 17.8	60.6 ± 15.5	71.0 ± 21.7	84.5 ± 23.2	103.5 ± 29.9	122.2 ± 34.5

Data for each subject are means ± SD for 39 lamellae.

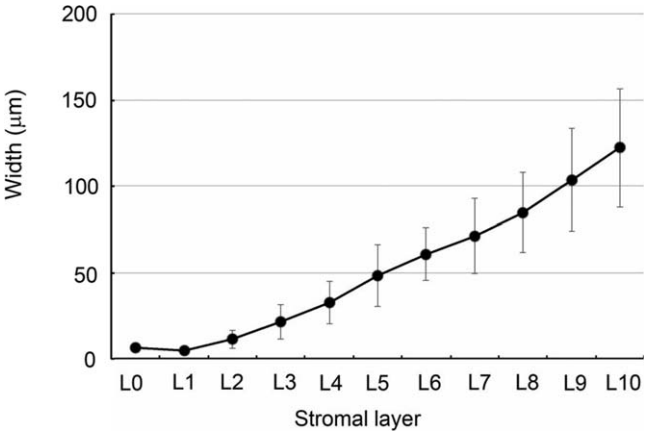

FIGURE 3. Width of collagen lamellae throughout the full thickness of the normal corneal stroma. L0 corresponds to collagen lamellae adherent to Bowman's layer. Data are means ± SD for 39 lamellae in 13 corneas.

software (Zeiss). Three data sets were collected from different randomly scanned regions of each corneal block.

Measurement of the Angle of Collagen Lamellae

The continuous SHG images derived from determined optical slices allowed the *z*-axis distance between two points to be obtained from the number of planes (distance *a*), and ZEN software provides the 3D distance between two points of interest (distance *b*). The angle (θ) of collagen lamellae relative to Bowman's layer was thus provided by $\theta = \sin^{-1}(a/b)$ (Fig. 1). We reviewed the data sets for each normal corneal specimen and divided them into 10 layers of equal depth, with layer 1 (L1) adjacent to Bowman's layer and L10 adjacent to Descemet's membrane. With this approach, each layer is ~50 μm in depth. We then identified the initiation and termination points of collagen lamellae in each layer, measured the *xy* distance between these two points for each lamella, and counted the number of *xy* slices. We measured the angle of 39 different collagen lamellae in each layer for each of the three scanned regions of each tissue block. The total number of evaluated lamellae was thus 117 for each layer of the corneal stroma. For the keratoconic corneal specimens, the angle and width of collagen lamellae were measured at 50-μm-depth intervals of the corneal stroma, which approximately correspond to the layer intervals for the normal corneal specimens.

Measurement of the Width of Collagen Lamellae

We measured the width of collagen lamellae in each layer of the normal or keratoconic corneal stroma by moving the focal plane of the SHG data sets and with the use of ZEN software. The width of 13 lamellae in each layer of normal subjects was determined for each of the three scanned regions of each tissue block. The total number of evaluated lamellae was thus 39 for each layer of the corneal stroma.

Statistical Analysis

Quantitative data are presented as means ± SD. Differences in the angle and width of collagen lamellae between normal and keratoconic corneas were evaluated with Student's *t*-test. A P value < 0.05 was considered statistically significant.

TABLE 2. Angle of Collagen Lamellae (Degrees) in Normal Subjects

Age/Sex	L1	L2	L3	L4	L5	L6	L7	L8	L9	L10
48/F	19.6 ± 8.0	11.2 ± 4.9	8.5 ± 4.1	5.3 ± 2.3	5.3 ± 2.6	4.9 ± 2.0	4.8 ± 1.9	4.3 ± 1.9	3.9 ± 2.2	3.8 ± 3.3
57/M	18.2 ± 7.7	9.0 ± 4.0	3.4 ± 2.1	3.7 ± 1.6	3.8 ± 2.1	3.5 ± 2.3	3.4 ± 2.4	3.5 ± 2.4	3.6 ± 2.4	3.6 ± 3.0
57/M	22 ± 3.1	13.8 ± 4.4	6.0 ± 2.9	3.1 ± 3.1	2.1 ± 1.5	1.7 ± 1.5	1.9 ± 1.1	1.8 ± 0.9	1.4 ± 1.4	2.0 ± 1.2
65/M	27.2 ± 8.7	7.6 ± 2.9	5.4 ± 2.7	3.5 ± 2.2	2.4 ± 2.9	2.8 ± 2.9	2.0 ± 2.2	2.7 ± 2.0	1.8 ± 1.7	2.3 ± 1.5
68/M	18.5 ± 5.5	11.4 ± 3.8	9.0 ± 1.5	5.9 ± 1.7	5.3 ± 1.0	5.8 ± 1.0	4.4 ± 1.2	3.6 ± 0.6	3.4 ± 1.1	2.6 ± 0.5
69/F	22.2 ± 2.9	10.7 ± 2.5	7.4 ± 2.1	3.9 ± 1.0	4.0 ± 0.8	2.8 ± 0.6	3.2 ± 3.5	2.5 ± 2.3	2.4 ± 2.4	1.6 ± 1.5
69/M	24.6 ± 7.9	11.0 ± 3.2	8.7 ± 3.0	8.0 ± 2.6	5.7 ± 2.4	5.0 ± 2.0	4.4 ± 2.6	4.2 ± 3.1	3.4 ± 2.6	2.7 ± 2.2
43/F	17.4 ± 2.2	8.1 ± 2.9	5.2 ± 1.2	4.0 ± 0.5	4.1 ± 0.6	4.2 ± 0.6	4.8 ± 0.9	3.8 ± 0.4	4.2 ± 0.9	3.1 ± 1.1
69/M	21.1 ± 1.7	9.2 ± 2.9	7.2 ± 2.1	4.3 ± 1.5	3.0 ± 1.0	3.7 ± 0.3	2.3 ± 0.6	3.5 ± 1.0	3.5 ± 0.1	2.5 ± 0.4
63/F	20.0 ± 1.7	11.6 ± 2.7	5.5 ± 2.0	4.7 ± 1.7	3.7 ± 1.2	2.9 ± 1.2	2.3 ± 1.0	1.7 ± 0.7	1.3 ± 0.8	0.9 ± 0.7
48/F	19.2 ± 2.5	12.2 ± 3.2	7.2 ± 2.6	6.1 ± 1.4	5.2 ± 1.5	4.7 ± 2.6	4.2 ± 0.7	5.5 ± 1.0	4.7 ± 0.9	5.3 ± 1.1
75/F	22.4 ± 5.7	11.9 ± 3.2	9.7 ± 0.4	6.3 ± 3.0	5.5 ± 2.2	5.3 ± 1.5	6.7 ± 1.1	4.4 ± 2.6	2.9 ± 2.2	3.8 ± 1.5
69/F	19.2 ± 8.8	9.8 ± 1.2	3.4 ± 0.8	2.8 ± 3.6	1.4 ± 1.7	1.4 ± 0.3	1.3 ± 0.4	0.8 ± 0.7	2.0 ± 1.1	1.2 ± 1.3
Overall mean ± SD	20.9 ± 5.4	10.6 ± 3.2	6.7 ± 2.8	4.7 ± 2.5	4.0 ± 2.1	3.7 ± 2.1	3.5 ± 1.9	3.3 ± 2.0	3.0 ± 2.0	2.7 ± 2.2

Data for each subject are means ± SD for 117 lamellae.

FIGURE 4. Depth profile for the angle of collagen lamellae relative to Bowman's layer in the normal corneal stroma. Data are means ± SD for 117 lamellae in 13 corneas.

RESULTS

Second harmonic generation imaging microscopy allows visualization of collagen fibrils and lamellae in coronal sections parallel to the surface of the cornea. Consistent with our previous observations,[6,7,23] collagen signals derived from the anterior stroma of the normal human cornea revealed short collagen fibrils in random orientations, whereas those derived from the middle or posterior stroma revealed bundles of wider and longer collagen fibrils also in random orientations (Fig. 2A). From the collected data sets, we reconstructed 3D images of collagen lamellae (Fig. 2B) as well as corresponding projection images (Fig. 2C) for the entire thickness of the corneal stroma. The reconstructed projection images revealed interwoven narrow collagen lamellae oriented at a relatively steep angle relative to Bowman's layer in the anterior stroma, as well as wider and flatter lamellae oriented relatively parallel to Bowman's layer in the middle and posterior stroma.

From such images, we measured the width of collagen lamellae in 10 assigned layers of the normal corneal stroma between Bowman's layer and Descemet's membrane (L1–L10), as well as of those adherent to Bowman's layer (L0) (Table 1; Fig. 3). The mean width ± SD of collagen lamellae at L0 was 6.5 ± 1.7 μm (range, 2.4–11.2), whereas that in L1 (the layer adjacent to Bowman's layer) was smaller at 4.3 ± 1.3 μm (range, 2.1–7.9). The width of the lamellae then gradually increased with tissue depth, consistent with our previous observations for the anterior stroma.[7] The corresponding values for L2 to L10 were thus 11.2 ± 5.3 μm (range, 3.3–24.1), 21.3 ± 10.3 μm (range, 4.9–57.0), 32.6 ± 12.4 μm (range, 5.1–55.9), 48.0 ± 17.8 μm (range, 11.0–85.1), 60.6 ± 15.5 μm (range, 30.6–97.5), 71.0 ± 21.7 μm (range, 35.3–111.6), 84.5 ± 23.2 μm (range, 47.3–136.8), 103.5 ± 29.9 μm (range, 67.8–188.3), and 122.2 ± 34.5 μm (range, 69.1–232.0), respectively. We also measured the angle of collagen lamellae in each layer relative to Bowman's layer (Table 2; Fig. 4). The angle (mean ± SD) of collagen lamellae adjacent to Bowman's layer (in L1) was 20.9° ± 5.4° (range, 10.5°–42.5°), whereas the angle of those in L2 decreased to 10.6° ± 3.2° (range, 4.4°–21.0°) and that of those in L3 to L10 then decreased gradually to 6.7° ± 2.8° (range, 0.4°–12.5°), 4.7° ± 2.5° (range, 0.1°–10.4°), 4.0° ± 2.1° (range, 0.1°–8.8°), 3.7° ± 2.1° (range, 0.0°–8.6°), 3.5° ± 1.9° (range, 0.2°–8.6°), 3.3° ± 2.0° (range, 0.1°–10.6°), 3.0° ± 2.0° (range, 0.1°–7.1°), and 2.7° ± 2.2° (range, 0.0°–9.6°), respectively. This decrease in the angle of collagen lamellae with distance from Bowman's layer is also consistent with our previous observations for the anterior stroma.[7]

TABLE 3. Width of Collagen Lamellae (μm) in Keratoconic Subjects

Age/Sex	C or M-P	L1	L2	L3	L4	L5	L6	L7	L8	L9	L10
63/F	C	4.4 ± 1.1	12.9 ± 7.4	41.7 ± 38.3	77.5 ± 67.4	113.2 ± 78.7	133.2 ± 11.1*	216.0 ± 20.3†	-	-	-
	M-P	3.1 ± 0.2†	15.1 ± 5.3	34.1 ± 8.4	58.1 ± 12.8	65.7 ± 11.0*	91.9 ± 22.9	120.4 ± 40.4	150.2 ± 42.5†	-	-
41/M	C	9.8 ± 5.5	29.5 ± 19.1	66.5 ± 45.7	168.0 ± 36.3†	-	-	-	-		
	M-P	8.0 ± 1.1*	19.0 ± 4.4	36.9 ± 9.3	60.6 ± 11.5*	73.0 ± 21.3	83.3 ± 17.1	107.5 ± 8.9	143.4 ± 7.9†	-	-
38/M	C	4.1 ± 1.8	10.2 ± 6.4	48.7 ± 27.5*	85.4 ± 20.8†	-	-	-	-	-	-
	M-P	6.6 ± 1.5†	10.4 ± 2.0	25.1 ± 6.7*	73.4 ± 22.0†	101.0 ± 18.9†	117.9 ± 19.5†	122.6 ± 32.6†	-	-	-
64/F	C	5.7 ± 1.4*	14.4 ± 8.6	21.9 ± 11.3	44.3 ± 25.3	87.0 ± 24.7†	97.4 ± 18.0†	128.8 ± 37.1†	-	-	-
	M-P	4.2 ± 1.3	7.8 ± 3.6	9.1 ± 6.0*	23.4 ± 6.2*	54.7 ± 14.3*	83.9 ± 9.8†	111.5 ± 36.2†	125.7 ± 34.5†	139.3 ± 25.4†	131.6 ± 26.2*

Data are means ± SD for 9 lamellae. C or M-P, central or midperipheral region of the cornea, respectively.

* $P < 0.05$.

† $P < 0.01$ versus corresponding overall mean value for the normal cornea (unpaired Student's *t*-test).

We also similarly evaluated corneal specimens from four individuals with keratoconus (Figs. 2D–F). The width of collagen lamellae in each keratoconic cornea was similar to that in the normal cornea at the anterior stroma but increased to a greater extent with tissue depth (Table 3; Figs. 5A–D). In addition, the collagen lamellae in the central region of each keratoconic cornea were wider than those in the midperipheral region. Statistical analysis revealed that the width of collagen lamellae in the mid to posterior stroma of each keratoconic cornea was significantly larger than that in the normal cornea, although there was substantial interindividual variability (Table 3). Compared with the normal cornea, the angle of collagen lamellae relative to Bowman's layer tended to be flatter and to decrease to a lesser extent with tissue depth in the keratoconic cornea (Table 4; Figs. 5E–H). The angle also tended to be flatter in the central region of the keratoconic cornea than in the midperipheral region. Statistical analysis revealed that the angle of collagen lamellae at the anterior stroma of each keratoconic cornea was significantly flatter than that in the normal cornea (Table 4). The width and angle of collagen lamellae in the central region of the keratoconic cornea thus differed from those in the normal cornea to a greater extent than did those in the midperipheral region of the keratoconic cornea.

DISCUSSION

We have here determined the structural characteristics of collagen lamellae throughout the stroma of the normal and keratoconic human cornea. Our data reveal that collagen lamellae at the anterior stroma of the normal cornea are interwoven in three dimensions, and that they are wider and form a flatter angle with Bowman's layer compared with the textbook description.[24] These characteristics of collagen lamellae were found to be dependent on stromal depth. Furthermore, in the keratoconic cornea, collagen lamellae were wider and formed a flatter angle with Bowman's layer than in the normal cornea. These differences in the structure of collagen lamellae between the normal and keratoconic cornea may be related to the change in anterior corneal shape characteristic of individuals with keratoconus.

We measured the angle of collagen lamellae relative to Bowman's layer at various distances between Bowman's layer and Descemet's membrane. Collagen lamellae in the corneal stroma have previously been described as parallel to each other,[24] with those in the anterior stroma being oblique and inserted into Bowman's layer.[25–27] The characteristics of collagen lamellae in the anterior one-third of the corneal stroma were also previously found to differ from those of lamellae in the posterior two-thirds.[28] Indeed, it has been suggested that the embryonic origin of the anterior stroma differs from that of the posterior stroma.[29] Our quantitative analysis has now shown that the angle of collagen lamellae in the anterior one-third (L1–L4) of the normal human corneal stroma is steeper than that of those in the posterior two-thirds.

We also measured the width of collagen lamellae throughout the entire thickness of the normal human corneal stroma. The lamellae anchored at Bowman's layer were wider than those otherwise adjacent to Bowman's layer, after which the width of the lamellae increased gradually with distance toward Descemet's membrane. The width of collagen lamellae in the normal human corneal stroma was previously found by light microscopy to range from 9 to 250 μm,[24] whereas subsequent electron microscopic analysis determined the range to be 0.5 to 250 μm.[2] Our data now show

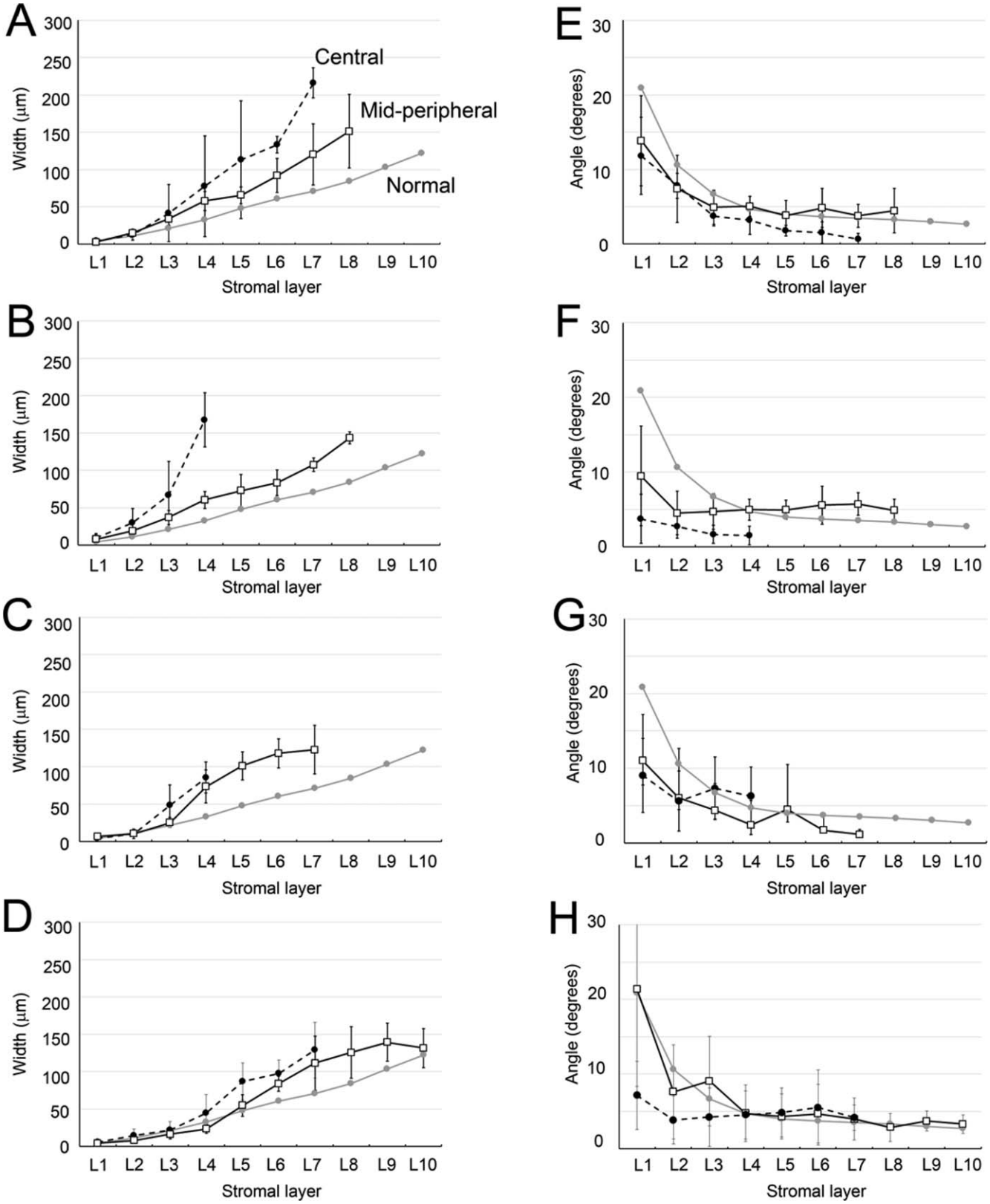

FIGURE 5. Width (**A**–**D**) and angle (**E**–**H**) profiles for collagen lamellae in the keratoconic corneal stroma. *Closed black circles* and *open squares*, collagen lamellae in the central and midperipheral regions, respectively, for each of four keratoconic corneas; *closed gray circles*, collagen lamellae in the normal cornea as shown in Figures 3 and 4. The keratoconic corneal specimens were obtained from a 63-year-old woman (**A**, **E**), a 41-year-old man (**B**, **F**), a 38-year-old man (**C**, **G**), and a 64-year-old woman (**D**, **H**). Data for each keratoconic specimen are means ± SD for 39 (width) or 117 (angle) lamellae.

TABLE 4. Angle of Collagen Lamellae (Degrees) in Keratoconic Subjects

Age/Sex	C or M-P	L1	L2	L3	L4	L5	L6	L7	L8	L9	L10
63/F	C	11.8 ± 5.2†	7.8 ± 1.7†	3.7 ± 1.3†	3.2 ± 1.8*	1.8 ± 0.7†	1.5 ± 1.4*	0.7 ± 0.7†	-	-	-
	M-P	13.9 ± 6.0†	7.4 ± 4.5	4.9 ± 2.3	5.1 ± 1.3	3.8 ± 2.0	4.8 ± 2.6	3.8 ± 1.6	4.8 ± 2.9	-	-
41/M	C	3.7 ± 3.3†	2.7 ± 1.5†	1.7 ± 1.2†	1.4 ± 1.2†	-	-	-	-	-	-
	M-P	9.5 ± 6.7†	4.5 ± 2.9†	4.7 ± 2.4*	5.0 ± 1.4	5.0 ± 1.3	5.6 ± 2.6	5.7 ± 1.5*	5.0 ± 1.5*	-	-
38/M	C	9.0 ± 5.0†	5.6 ± 4.0†	7.3 ± 4.2	6.3 ± 3.9	-	-	-	-	-	-
	M-P	11.0 ± 6.1†	6.0 ± 6.6	4.4 ± 3.6	2.4 ± 3.3	4.5 ± 6.0	1.7 ± 2.1*	1.1 ± 0.7†	-	-	-
64/F	C	7.1 ± 4.6†	3.9 ± 3.2†	4.2 ± 3.9	4.5 ± 3.2	4.9 ± 3.3	5.5 ± 5.1	4.2 ± 1.7	-	-	-
	M-P	21.4 ± 13.0	7.6 ± 6.3	9.6 ± 5.7	4.8 ± 3.8	4.3 ± 3.0	4.7 ± 3.9	4.0 ± 2.8	2.9 ± 1.9	3.7 ± 1.4	3.3 ± 1.2

Data are means ± SD for 9 lamellae. C or M-P, central or midperipheral region of the cornea, respectively.

* $P < 0.05$.

† $P < 0.01$ versus corresponding overall mean value for the normal cornea (unpaired Student's *t*-test).

that the width of the narrow collagen lamellae adjacent to Bowman's layer (L1) ranged from 2.1 to 7.9 μm, whereas that of the wide lamellae adjacent to Descemet's membrane (L10) ranged from 69.1 to 232.0 μm.

We found that collagen lamellae in the keratoconic cornea, especially in the central region, were wider and formed a smaller angle with Bowman's layer compared with those in the normal cornea. These findings may suggest that collagen lamellae in the keratoconic cornea are expanded in association with protrusion of the cone. Several previous studies have examined the properties of collagen fibrils and lamellae in the keratoconic cornea.[18,30–32] One previous study found that the structural characteristics of collagen fibrils and lamellae in the keratoconic cornea are altered, and that slippage of the fibrils and lamellae may give rise to protrusion of the cone.[19] Such slippage may result in widening of the collagen lamellae, consistent with our present data, and in consequent lateral expansion of the corneal stroma and protrusion of the cone. This lateral expansion of the corneal stroma may cause collagen lamellae to become packed or squashed, resulting in a flattening of the angle of the lamellae relative to Bowman's layer. We were not able to evaluate the interfibrillar space within collagen lamellae or the thickness of the lamellae because of the limited resolution of SHG imaging and the lack of an established measuring procedure, respectively. The detailed mechanism of corneal protrusion in keratoconus thus remains to be clarified.

Our quantitative analysis of the angle and width of collagen lamellae was enabled by the application of SHG imaging to whole-mount preparations of the human cornea. Such imaging does not require tissue sectioning and therefore maintains the 3D structure of corneal collagen,[33,34] and it has been widely applied to studies of the normal and diseased cornea.[6,7,22,23,35–38]

Our data support a clinical impression obtained during deep lamellar anterior keratoplasty (DALK). Our experience is that it is often difficult to remove the anterior portion of the corneal stroma with a surgical spatula, likely as a result of the highly interwoven nature of collagen lamellae in this region of the stroma and its consequent rigidity. In contrast, it is easier to separate the posterior stroma with unimpeded movement of the surgical spatula.

The presence of fine and interwoven collagen lamellae in the anterior stroma likely underlies structural rigidity at the surface of the eyeball and is thought to contribute to maintenance of anterior corneal curvature.[27] Fine lamellae in random orientations would be expected to confer rigidity in the direction parallel to Bowman's layer, whereas interwoven lamellae would be expected to confer rigidity in the perpendicular direction. The biomechanics of the corneal stroma have been investigated by measurement of pulling force[39,40] and corneal hysteresis,[41–43] as well as with Brillouin microscopy[44,45] and atomic force microscopy.[46–48] These studies have revealed that the anterior stroma is stiffer than the posterior stroma. The anterior stroma was also found not to swell in response to an artificial edema-inducing condition, indicating that the anterior stroma indeed contributes to maintenance of anterior corneal curvature.[49] A recent study found that the interwoven structure of collagen lamellae at the anterior stroma is associated with steeper angles of the lamellae compared with those of the less interwoven lamellae in the anterior-middle or middle stroma.[50] Our results are consistent with this latter finding and provide further support for the notion that the structural characteristics of collagen lamellae at the anterior stroma are key to the rigidity of this portion of the cornea. The specific properties conferred by the structural

characteristics of collagen lamellae at the posterior stroma remain to be determined.

Acknowledgments

The authors thank Akira Kobayashi for providing sclerocorneal specimens.

Disclosure: **N. Morishige**, None; **R. Shin-gyou-uchi**, None; **H. Azumi,** None; **H. Ohta**, None; **Y. Morita**, None; **N. Yamada**, None; **K. Kimura**, None; **A. Takahara**, None; **K.-H. Sonoda**, None

References

1. Drubaix I, Legeais JM, Malek-Chehire N, et al. Collagen synthesized in fluorocarbon polymer implant in the rabbit cornea. *Exp Eye Res*. 1996;62:367–376.
2. Komai Y, Ushiki T. The three-dimensional organization of collagen fibrils in the human cornea and sclera. *Invest Ophthalmol Vis Sci*. 1991;32:2244–2258.
3. Radner W, Zehetmayer M, Aufreiter R, Mallinger R. Interlacing and cross-angle distribution of collagen lamellae in the human cornea. *Cornea*. 1998;17:537–543.
4. Maurice D. The cornea and sclera. In: Davson H, ed. *The Eye*. New York: Academic Press; 1969:489–599.
5. Meek KM, Boote C. The organization of collagen in the corneal stroma. *Exp Eye Res*. 2004;78:503–512.
6. Morishige N, Petroll WM, Nishida T, Kenney MC, Jester JV. Noninvasive corneal stromal collagen imaging using two-photon-generated second-harmonic signals. *J Cataract Refract Surg*. 2006;32:1784–1791.
7. Morishige N, Takagi Y, Chikama T, Takahara A, Nishida T. Three-dimensional analysis of collagen lamellae in the anterior stroma of the human cornea visualized by second harmonic generation imaging microscopy. *Invest Ophthalmol Vis Sci*. 2011;52:911–915.
8. Saghizadeh M, Chwa M, Aoki A, et al. Altered expression of growth factors and cytokines in keratoconus, bullous keratopathy and diabetic human corneas. *Exp Eye Res*. 2001;73:179–189.
9. Jun AS, Cope L, Speck C, et al. Subnormal cytokine profile in the tear fluid of keratoconus patients. *PloS One*. 2011;6:e16437.
10. Smith VA, Easty DL. Matrix metalloproteinase 2: involvement in keratoconus. *Eur J Ophthalmol*. 2000;10:215–226.
11. Saghizadeh M, Brown DJ, Castellon R, et al. Overexpression of matrix metalloproteinase-10 and matrix metalloproteinase-3 in human diabetic corneas: a possible mechanism of basement membrane and integrin alterations. *Am J Pathol*. 2001;158:723–734.
12. Balasubramanian SA, Pye DC, Willcox MD. Are proteinases the reason for keratoconus? *Curr Eye Res*. 2010;35:185–191.
13. Kenney MC, Chwa M, Atilano SR, et al. Increased levels of catalase and cathepsin V/L2 but decreased TIMP-1 in keratoconus corneas: evidence that oxidative stress plays a role in this disorder. *Invest Ophthalmol Vis Sci*. 2005;46:823–832.
14. Chwa M, Atilano SR, Hertzog D, et al. Hypersensitive response to oxidative stress in keratoconus corneal fibroblasts. *Invest Ophthalmol Vis Sci*. 2008;49:4361–4369.
15. Arnal E, Peris-Martinez C, Menezo JL, Johnsen-Soriano S, Romero FJ. Oxidative stress in keratoconus? *Invest Ophthalmol Vis Sci*. 2011;52:8592–8597.
16. Sawaguchi S, Fukuchi T, Abe H, Kaiya T, Sugar J, Yue BY. Three-dimensional scanning electron microscopic study of keratoconus corneas. *Arch Ophthalmol*. 1998;116:62–68.
17. Radner W, Zehetmayer M, Skorpik C, Mallinger R. Altered organization of collagen in the apex of keratoconus corneas. *Ophthalmic Res*. 1998;30:327–332.
18. Akhtar S, Bron AJ, Salvi SM, Hawksworth NR, Tuft SJ, Meek KM. Ultrastructural analysis of collagen fibrils and proteoglycans in keratoconus. *Acta Ophthalmol*. 2008;86:764–772.
19. Meek KM, Tuft SJ, Huang Y, et al. Changes in collagen orientation and distribution in keratoconus corneas. *Invest Ophthalmol Vis Sci*. 2005;46:1948–1956.
20. Hayes S, Boote C, Tuft SJ, Quantock AJ, Meek KM. A study of corneal thickness, shape and collagen organisation in keratoconus using videokeratography and X-ray scattering techniques. *Exp Eye Res*. 2007;84:423–434.
21. Lo W, Chen WL, Hsueh CM, et al. Fast Fourier transform-based analysis of second-harmonic generation image in keratoconic cornea. *Invest Ophthalmol Vis Sci*. 2012;53:3501–3507.
22. Tan HY, Sun Y, Lo W, et al. Multiphoton fluorescence and second harmonic generation imaging of the structural alterations in keratoconus ex vivo. *Invest Ophthalmol Vis Sci*. 2006;47:5251–5259.
23. Morishige N, Wahlert AJ, Kenney MC, et al. Second-harmonic imaging microscopy of normal human and keratoconus cornea. *Invest Ophthalmol Vis Sci*. 2007;48:1087–1094.
24. Hogan MJ, Alvarado JA, Weddell JE. The cornea. In: *Histology of the Human Eye*. Philadelphia: W.B. Saunders; 1971:55–111.
25. Polack FM. Morphology of the cornea. I. Study with silver stains. *Am J Ophthalmol*. 1961;51:1051–1056.
26. Tripathi RC, Bron AJ. Secondary anterior crocodile shagreen of Vogt. *Br J Ophthalmol*. 1975;59:59–63.
27. Bron AJ, Tripathi RC, Tripathi BJ. The cornea and sclera. In: *Wolff's Anatomy of the Eye and Orbit*. London: Chapman & Hall Medical; 1997:233–278.
28. McTigue JW. The human cornea: a light and electron microscopic study of the normal cornea and its alterations in various dystrophies. *Trans Am Ophthalmol Soc*. 1967;65:591–660.
29. Barishak YR. *Embryology of the Eye and Its Adnexae*. Basel: Karger; 2001:7–37.
30. Patey A, Savoldelli M, Pouliquen Y. Keratoconus and normal cornea: a comparative study of the collagenous fibers of the corneal stroma by image analysis. *Cornea*. 1984;3:119–124.
31. Fullwood NJ, Tuft SJ, Malik NS, Meek KM, Ridgway AE, Harrison RJ. Synchrotron x-ray diffraction studies of keratoconus corneal stroma. *Invest Ophthalmol Vis Sci*. 1992;33:1734–1741.
32. Takahashi A, Nakayasu K, Okisaka S, Kanai A. Quantitative analysis of collagen fiber in keratoconus [in Japanese]. *Nippon Ganka Gakkai Zasshi*. 1990;94:1068–1073.
33. Morishige N, Nishida T, Jester JV. Second harmonic generation for visualizing 3-dimensional structure of corneal collagen lamellae. *Cornea*. 2009;28:S46–S53.
34. Mohler W, Millard AC, Campagnola PJ. Second harmonic generation imaging of endogenous structural proteins. *Methods*. 2003;29:97–109.
35. Teng SW, Tan HY, Peng JL, et al. Multiphoton autofluorescence and second-harmonic generation imaging of the ex vivo porcine eye. *Invest Ophthalmol Vis Sci*. 2006;47:1216–1224.
36. Morishige N, Yamada N, Teranishi S, Chikama T, Nishida T, Takahara A. Detection of subepithelial fibrosis associated with corneal stromal edema by second harmonic generation imaging microscopy. *Invest Ophthalmol Vis Sci*. 2009;50:3145–3150.
37. Morishige N, Yamada N, Zhang X, et al. Abnormalities of stromal structure in the bullous keratopathy cornea identified

Investigative Ophthalmology & Visual Science

by second harmonic generation imaging microscopy. *Invest Ophthalmol Vis Sci*. 2012;53:4998–5003.

38. Morishige N, Sonoda KH. Bullous keratopathy as a progressive disease: evidence from clinical and laboratory imaging studies. *Cornea*. 2013;32(suppl 1):S77–S83.
39. Maurice DM, Monroe F. Cohesive strength of corneal lamellae. *Exp Eye Res*. 1990;50:59–63.
40. Richoz O, Kling S, Zandi S, Hammer A, Spoerl E, Hafezi F. A constant-force technique to measure corneal biomechanical changes after collagen cross-linking. *PloS One*. 2014;9: e105095.
41. Luce DA. Determining in vivo biomechanical properties of the cornea with an ocular response analyzer. *J Cataract Refract Surg*. 2005;31:156–162.
42. Shah S, Laiquzzaman M, Bhojwani R, Mantry S, Cunliffe I. Assessment of the biomechanical properties of the cornea with the ocular response analyzer in normal and keratoconic eyes. *Invest Ophthalmol Vis Sci*. 2007;48:3026–3031.
43. Moreno-Montanes J, Maldonado MJ, Garcia N, Mendiluce L, Garcia-Gomez PJ, Segui-Gomez M. Reproducibility and clinical relevance of the ocular response analyzer in nonoperated eyes: corneal biomechanical and tonometric implications. *Invest Ophthalmol Vis Sci*. 2008;49:968–974.
44. Scarcelli G, Kling S, Quijano E, Pineda R, Marcos S, Yun SH. Brillouin microscopy of collagen crosslinking: noncontact depth-dependent analysis of corneal elastic modulus. *Invest Ophthalmol Vis Sci*. 2013;54:1418–1425.
45. Scarcelli G, Besner S, Pineda R, Yun SH. Biomechanical characterization of keratoconus corneas ex vivo with Brillouin microscopy. *Invest Ophthalmol Vis Sci*. 2014;55:4490–4495.
46. Lombardo M, Lombardo G, Carbone G, De Santo MP, Barberi R, Serrao S. Biomechanics of the anterior human corneal tissue investigated with atomic force microscopy. *Invest Ophthalmol Vis Sci*. 2012;53:1050–1057.
47. Last JA, Thomasy SM, Croasdale CR, Russell P, Murphy CJ. Compliance profile of the human cornea as measured by atomic force microscopy. *Micron*. 2012;43:1293–1298.
48. Dias JM, Ziebarth NM. Anterior and posterior corneal stroma elasticity assessed using nanoindentation. *Exp Eye Res*. 2013; 115:41–46.
49. Muller LJ, Pels E, Vrensen GF. The specific architecture of the anterior stroma accounts for maintenance of corneal curvature. *Br J Ophthalmol*. 2001;85:437–443.
50. Winkler M, Shoa G, Xie Y, et al. Three-dimensional distribution of transverse collagen fibers in the anterior human corneal stroma. *Invest Ophthalmol Vis Sci*. 2013;54:7293–7301.

Investigative Ophthalmology & Visual Science